Bioactive Materials 2 (2017) 177–184

Contents lists available at ScienceDirect

Bioactive Materials

journal homepage: http://www.keaipublishing.com/en/journals/bioactive-materials/

Comparative investigations of structure and properties of micro-arc wollastonite-calcium phosphate coatings on titanium and zirconium-niobium alloy

M.B. Sedelnikova [a, *], E.G. Komarova [a], Yu.P. Sharkeev [a, b], T.V. Tolkacheva [a], I.A. Khlusov [b, c, d], L.S. Litvinova [d], K.A. Yurova [d], V.V. Shupletsova [d]

[a] Institute of Strength Physics and Materials Science of SB RAS, Academicheskii pr., 2/4, 634055, Tomsk, Russia
[b] National Research Tomsk Polytechnic University, Lenina pr., 30, 634050, Tomsk, Russia
[c] Siberian State Medical University, 2 Moskovsky tr., 634050, Tomsk, Russia
[d] Immanuel Kant Baltic Federal University, 14 A. Nevskogo st., 236041, Kaliningrad, Russia

ARTICLE INFO

Article history:
Received 13 December 2016
Accepted 23 January 2017
Available online 13 February 2017

Keywords:
Micro-arc oxidation
Biocoatings
Calcium phosphate
Wollastonite

ABSTRACT

Investigation results of micro-arc wollastonite–calcium phosphate (W–CaP) biocoatings on the pure titanium (Ti) and Zr–1wt.%Nb (Zr–1Nb) alloy were presented. The voltages of 150–300 V generate the micro-arc oxidation (MAO) process with the initial amplitude current of 150–550 A and 100–350 A for Ti and Zr–1Nb substrates, respectively. The identical dependencies of changes of the coating thickness, surface roughness and adhesion strength on the process voltage were revealed for the both substrates. The W–CaP coatings with the thickness of 10–11 μm were formed on Ti and Zr–1Nb under the low process voltage of 130–150 V. Elongated wollastonite particles with the size in the range of 40–100 μm were observed in such coatings. The structure of the coatings on Ti was presented by the X–ray amorphous and crystalline phases. The X–ray reflexes relating to the crystalline phases of Ti and wollastonite were observed only in XRD patterns of the coatings deposited under 130–200 V on Ti. While, the crystalline structure with phases of $CaZr_4(PO_4)_6$, β–ZrP_2O_7, ZrO_2, and Zr was detected in the coatings on Zr–1Nb. FT–IRS, XRD, SEM, and TEM data confirmed that the increase of the process voltage to 300 V leads to the dissociation of the wollastonite. No toxic effect of specimens on a viability, morphology and motility of human adipose–derived multipotent mesenchymal stem cells was revealed *in vitro*.

1. Introduction

The most commonly used alloys in medicine are commercially pure titanium Grade 2 and Grade 4, titanium alloys Ti–6Al–4V, Ti–6Al–4V Eli, and vanadium–free alloys as Ti–6Al–7Nb and Ti–6Al–2.5Fe. However, preferred alloys without any toxic alloying elements, such as A1, V, Mo and others [1,2] that could affect the organism. In this case, the most perspective ones are valve bioinert metals – Ti, Zr, Nb, Hf, Ta and their alloys. The main advantages of these materials are good biocompatibility, hypotoxicity, high corrosion resistance, low thermal linear expansion, low thermal conductivity, non–magnetization, and insignificant specific weight. Commercially pure Ti is the most common material used for manufacturing of orthopedic and dental implants. However, low mechanical strength properties, especially low ultimate strength, limit the further application of pure titanium as implant material. In this case, the zirconium doped with niobium alloys were widely used in medicine due to the high mechanical properties as a result of primarily solid solution hardening. The Zr-1Nb and Zr-2.5Nb alloys have complex properties such as biocompatibility, low thermal conductivity, high fatigue strength and high corrosion resistance that provide their application as implant material [3].

* Corresponding author.
E-mail addresses: smasha5@yandex.ru (M.B. Sedelnikova), katerina@ispms.tsc.ru (E.G. Komarova), sharkeev@ispms.tsc.ru (Yu.P. Sharkeev), tolkacheva@ispms.tsc.ru (T.V. Tolkacheva), khlusov63@mail.ru (I.A. Khlusov), larisalitvinova@yandex.ru (L.S. Litvinova), kristina_kofanova@mail.ru (K.A. Yurova), vshupletsova@mail.ru (V.V. Shupletsova).

Peer review under responsibility of KeAi Communications Co., Ltd.

http://dx.doi.org/10.1016/j.bioactmat.2017.01.002

However, there is the problem of the acceptance of metallic implants in the human body. The solution to this problem is the applications of calcium phosphate (CaP) coatings which has a positive effect on living organism and stimulate the regeneration of bone tissue.

Micro-arc oxidation (MAO) also known as plasma electrolytic oxidation (PEO) is a relatively new technique of the surface treatment based on anodic oxidation, which became well-known for its ability to form *in situ* grown porous and homogeneous oxide coatings on such metals as Ti, Al, Mg, Nb, Zr and their alloys. Additionally, it is one of the most effective methods to modify the metallic surface by the CaP coating formation for the best biocompatibility and bioactivity [4–6]. Besides, the application of micro-arc treatment allows to deposit biocompatible coating with gradient structure, rough and porous morphology [5]. The surface properties of the implant such as surface topography, chemical and phase composition determine its interactions with the surrounding host tissue and are of prime importance for better cell adhesion, spreading and proliferation [7,8].

MAO modification of Ti, Mg, and their alloys has been extensively investigated [4,5,9], whereas studies of MAO modification of Zr and its alloys are still quite limited [6,10–12]. It was demonstrated by Ref. [11], that depending on the anodic oxidation conditions for deposition of oxide coatings on Zr, i.e. voltage, current density, electrolyte composition and temperature, it is possible to grow of oxide layers with thickness of several hundred nanometers. Galvanostatic anodic oxidation of Zr in sulphuric acid leads to stress-induced oxide breakdown under voltages above 120 V. To obtain the layers with higher concentrations of bioactive compounds, the MAO process can be performed in suspensions [13]. The addition of hydroxyapatite (HA), wollastonite (W), tricalcium phosphate (TCP), silica and other bioactive powders into electrolyte may enrich the coatings. A. Kazek-Kęsik and research group [14,15] proposed to add the wollastonite ($CaSiO_3$), and silica (SiO_2) into the electrolyte to deposit the bioactive coatings on Ti–15Mo and Ti–13Nb–13Zr alloy by PEO method. They showed that wollastonite embedded in the coatings provides their improved biological activity. The possibility of the formation of wollastonite-calcium phosphate (W–CaP) coatings on Ti and Ti-40 wt%Nb alloy by the MAO method was shown in our previous reports [16,17].

This paper presents the results of comparative investigations of the structure and properties of wollastonite–calcium phosphate coatings deposited by the MAO method on Ti and Zr–1wt.%Nb (Zr–1Nb) alloy.

2. Materials and methods

Commercially pure titanium (99.58 Ti, 0.12 O, 0.18 Fe, 0.07 C, 0.04 N, 0.01 H wt%) and Zr–1Nb alloy (96.54 Zr, 1.0 Nb, 0.32 Mo, 0.02 Si, 0.1 W, 0.29 Fe, 0.88 Ti, 0.1 O wt%) were used as substrates. The size of the samples was 10 × 10 × 1 mm^3. Samples were prepared with silicon–carbide paper of 120, 480, 600, 1200 grit, in series. Then samples were ultrasonically cleaned for 10 min in distilled water. The average roughness (*Ra*) of the samples was 0.3–0.5 μm. In order to carry out the MAO method the Micro–Arc 3.0 technique was used as in previous works [5,18]. The installation consists of a pulsed power source, galvanic bath with water cooling system, molibdenum electrodes, and software for controlling the deposition process. The electrolyte solution was prepared based on 30% phosphoric acid (H_3PO_4) with pH = 1–2. Then the hydroxyapatite ($Ca_{10}(PO_4)_6(OH)_2$) and wollastonite ($CaSiO_3$) powders were added into the electrolyte in amount of 60 g/l and 75 g/l, respectively. Hydroxyapatite (HA) particles were 10–50 nm in size, and wollastonite (W) particles were 5–100 μm in length with average length of 35 μm. As a result, the homogeneous electrolyte with an ultradispersed phase was produced. The MAO process was carried out with the following parameters: pulse frequency of 50 Hz, pulse duration in the range of 100–500 μs, electrical voltage in the range of 130–300 V, and process duration from 5 to 10 min.

The morphology and microstructure of the coatings were examined by scanning electron microscopy (SEM, Zeiss LEO EVO 50, Germany) and transmission electron microscopy (TEM, JEOL JEM–2100, Japan) in “Nanotech” center at ISPMS SB RAS. In addition, the elemental compositions and distributions of the coatings were analyzed using energy-dispersive X-ray spectroscopy (EDX, Pegasus XM2 and INCA, Oxford Instruments) in combination with the SEM systems. The phase composition was determined by X–ray diffraction analysis (XRD, DRON–7 “Nanotech” center) in the angular range of $2\theta = 10–95^\circ$ with a scan step of 0.02° with Co Kα radiation. Infrared spectra were measured with a Fourier transform infrared spectrophotometer (FT–IRS, BIO RAD FTS 175, Germany) in the wave number range of 400–4500 cm^{-1}. The surface roughness was estimated with a Hommel–Etamic T1000 profilometer (Jenoptik, Germany) by the average roughness (*Ra*). The traverse length and rate of the measured profile were 6 mm and 0.5 mm/s, respectively. To measure the coating adhesion strength to the substrates, two cylinders were glued by the Loctite Hysol 9514 glue to both sides of the coated specimen. The specimens were fixed by grips in the Instron–1185 machine (Instron, USA) for carrying out the tensile test. Adhesion strength was measured as $\sigma_A = F/S$, where *F* is the breakout force and *S* is the area of broken out coating from substrate [19].

Biological tests *in vitro* of specimens with coatings were carried out using human adipose–derived multipotent mesenchymal stem cells (AMMSCs). For biological tests the Ti and Zr-1Nb specimens with W-CaP coatings were dry–heat sterilized with Binder FD53 (Binder GmbH, Tuttlingen, Germany) at 453 K for 1 h. Single specimen per each well was placed in 12–well plastic plates (Orange Scientific, Belgium) with cell culture medium. The control group was a cell culture medium without tested specimens. The AMMSCs culture was prepared from human fat tissue after processing of lipoaspirates (Permission No. 4 from 23.10.2013 of Local Ethics Committee of Innovation Park of Immanuel Kant Baltic Federal University) as particularly described by Ref. [20]. The cell suspension was freshly prepared with a concentration of 5 × 10^4 viable karyocytes/mL of the following culture medium: 90% DMEM/F12 (1:1) (Gibco Life Technologies; Grand Island, NY, USA), 10% fetal bovine serum (Sigma–Aldrich, St. Louis, MO, USA), 50 mg/l gentamicin (Invitrogen, UK) and freshly added L–glutamine sterile solution in a final concentration of 280 mg/l (Sigma–Aldrich). The cell culture was incubated for 7 days in a humidified atmosphere of 95% air and 5% CO_2 at 37 °C. The morphology of adherent cells, their motility and ability to form a monolayer in contact (in the interface) with the tested specimens was studied using integrated platforms for continuous visualization of living cells Cell–IQ® v2 MLF (CM Technologies, Finland). Digital images were obtained in 20 min during 7–day culturing. A viability of cells contacted *in vitro* with tested specimens was estimated by 0.4% trypan blue dyeing (Invitrogen, USA) according to ISO 10993-5 with the help of Countess ™ Automated Cell Counter (Invitrogen, USA). To determine a viability adherent AMMSCs were removed in 7 days from plastic wells by standard EDTA-trypsin processing and washed twice by culture medium.

3. Results and discussion

The influence of process voltage and substrate material on structure, morphology, thickness, roughness and adhesion strength of the W–CaP coatings were revealed. The graphs of amplitude current of the coating deposition against the MAO process duration

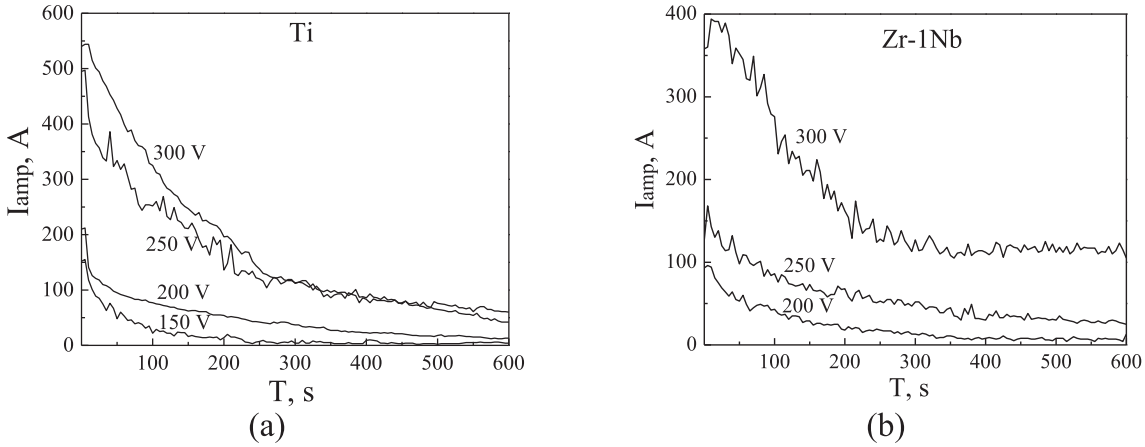

Fig. 1. Graphs of amplitude current of MAO process for deposition of W–CaP coatings on Ti (a) and Zr–1Nb (b) under different voltages.

for different voltages are observed in Fig. 1. With increasing of the applied voltage from 150 to 300 V the initial amplitude current grow in the ranges of 150–550 A and 100–400 A for Ti and Zr–1Nb, correspondingly. As a result, the current density grows and temperature of electrolyte increases from 20 to 40 °C. The amplitude current for Ti substrate is higher than for Zr–1Nb. It can be associated with the differences between physical properties of TiO_2 and ZrO_2 oxide films formed on Ti and Zr–1Nb, respectively. These oxides are forming during the MAO process in the intermediate layer between the metal substrate and the coating [5]. ZrO_2 has a lower dielectric capacitivity (18–21) and a higher band gap (6 eV) than TiO_2 (dielectric capacitivity of 30–100, and band gap of 3 eV) [5,18]. Character of the curves with the presence of amplitude current steps is connected with applied pulse voltage to the anode. The decrease of the current during the MAO process is due to the growth of dielectric W–CaP coatings on both substrates.

Fig. 2 illustrates the SEM-micrographs of W–CaP coatings deposited under the low process voltage of 130–150 V on Ti and Zr–1Nb. In this case, the thin coatings with thickness of 10–15 μm were formed. Elongated wollastonite particles with the size in the range of 40–100 μm are observed in SEM-images of the coating surface. Due to the large particle size the wollastonite crystals are not absolutely dissolved during the MAO process and can be involved into the coating. With increasing of the process voltage from 200 to 300 V spherical structural elements (spheres) with pores were formed on the coatings surface on the both substrates. The needle–like wollastonite crystals are not observed in this case (Fig. 3). This fact is confirmed by Fig. 4 which demonstrates the cross–sectional W–CaP coatings on both substrates deposited under different voltages. Thin W–CaP coating deposited at the 150 V on the Ti contains the wollastonite crystals (Fig. 4 a). However, the coatings deposited under voltages of 200–300 V on both substrates have porous structure with spherical elements on surface (Fig. 4 b–f).

EDX microanalysis recognizes that the large amount of Si is localized in the areas with needle-like particles in the coatings deposited under 150 V on Ti and Zr–1Nb (Fig. 5). It is evident that such particles correspond to the wollastonite crystals. However, these particles are not observed within the structure of the coatings formed under 200–300 V (Fig. 6). It can be a result of high temperatures in the micro–discharge areas promoted the dissociation of wollastonite crystals during the MAO process. In this case, the Si is distributed homogeneously throughout the coating.

Fig. 7 shows the dependencies of changes of the coating thickness, surface roughness and adhesion strength as the function of the voltage during the process of coating formation. The thickness of W–CaP coatings on the both substrates increases linearly from 10 to 110 μm with voltage increasing from 150 to 300 V (Fig. 7 a). It can be related to a current density growth and, as a consequence, to the increment of the coatings deposition rate [15]. In this case, the surface roughness of the W–CaP coatings on the both substrates increases from 1.5 to 7.0 μm (Fig. 7 b). The maximum adhesion strengths of 28 and 17 MPa were obtained for the coatings deposited under 150 V for 5 min on Ti and Zr–1Nb, respectively (Fig. 7 c). It is associated with the lowest thickness of such coatings. The increase of the oxidation voltage to 300 V leads to the decrease of the coating adhesion strength to 5–7 MPa [4].

XRD analysis has shown that the calcium phosphate substance of the coatings on Ti is in the X–ray amorphous state (Fig. 8 a). Two diffuse halo can be seen in XRD patterns in the angles range of

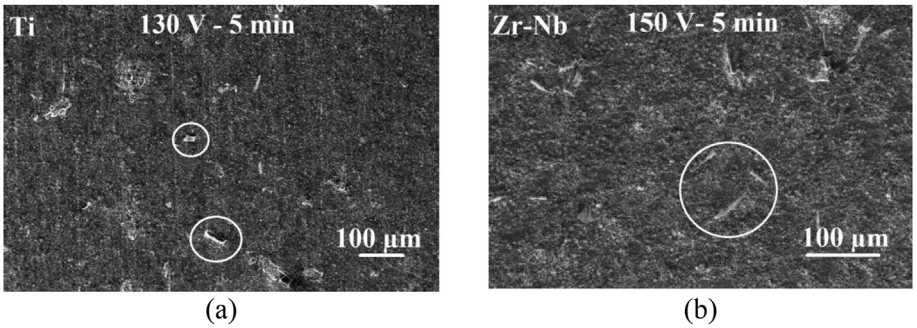

Fig. 2. SEM micrographs of the W–CaP coatings on Ti (a) and Zr–1Nb (b) produced under voltages of 130 and 150 V. The wollastanite crystals are marked by white circles.

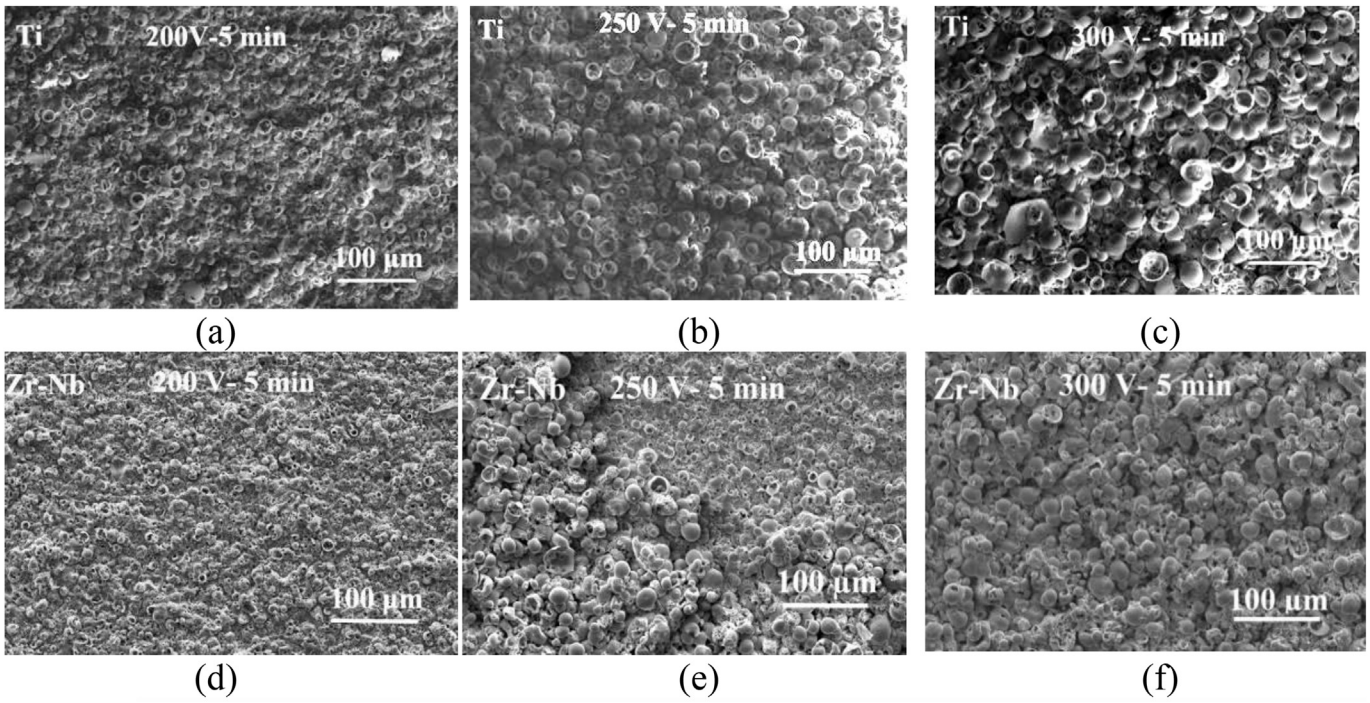

Fig. 3. SEM micrographs of the W–CaP coatings on Ti (a–c) and Zr–1Nb (d–f) produced under different voltages.

10–35°. Reflexes relating to wollastonite and Ti are observed only in XRD patterns of the thin coatings deposited under 150–200 V. However, peaks of the wollastonite are absent in XRD patterns of thicker coatings deposited under process voltages of 250–300 V. While, the W-CaP coatings on Zr–1Nb have the crystalline structure (Fig. 8 b, c). The phases of $CaZr_4(PO_4)_6$, β–ZrP_2O_7, ZrO_2–tetragonal and Zr substrate are detected. The coating formed on Zr–1Nb under low voltage of 150 V have a small thickness of 10 μm. Therefore the intense reflexes relating to the ZrO_2–tetragonal and Zr substrate are observed in XRD pattern of this coating

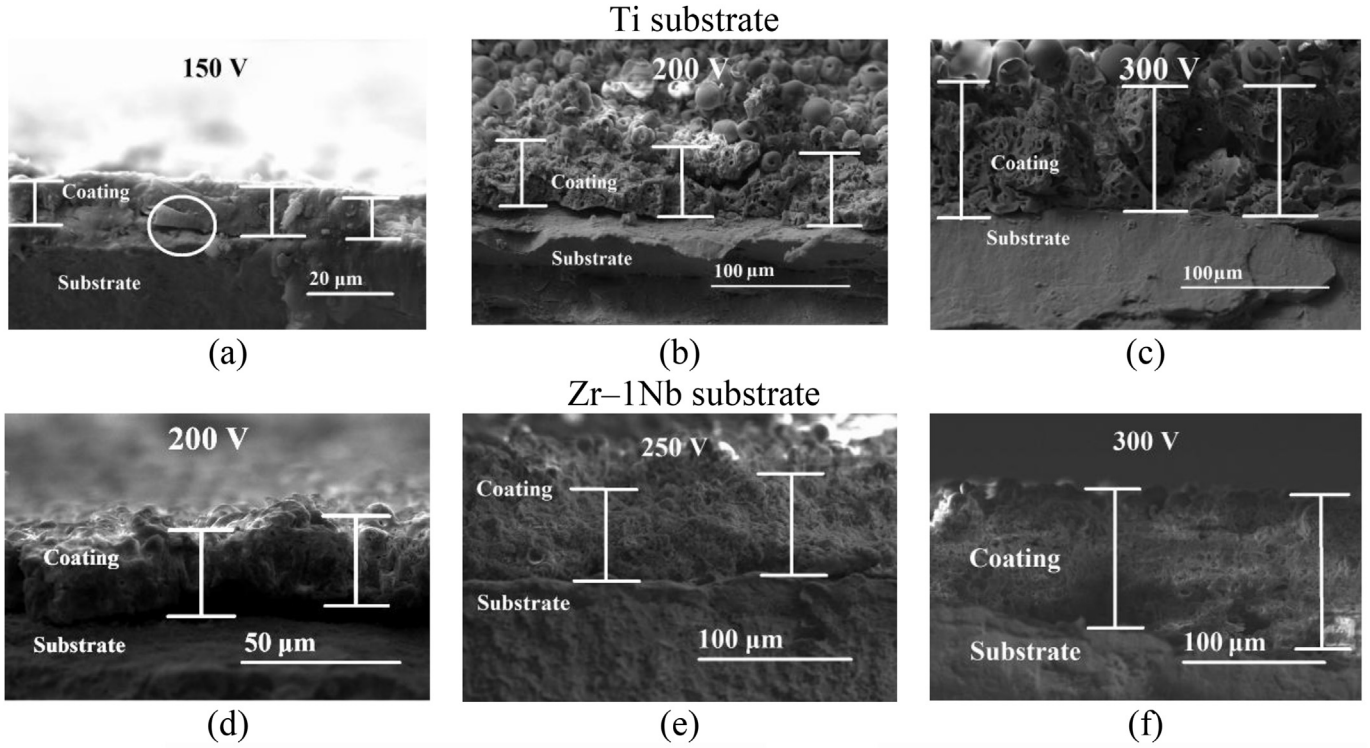

Fig. 4. SEM micrographs of the cross–sectional W–CaP coatings on Ti (a–c) and Zr–1Nb (d–f) produced under different voltages. The wollastanite crystals are marked by white circles.

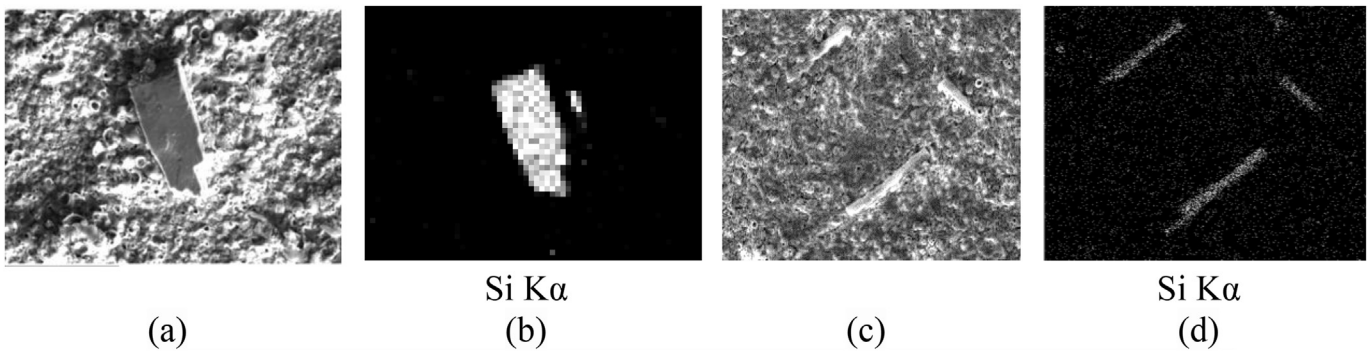

Fig. 5. SEM micrographs (a, c) and grey-level maps of Si distribution (b, d) in the W–CaP coating on Ti (a, b) and Zr–1Nb (c, d) produced under 150 V.

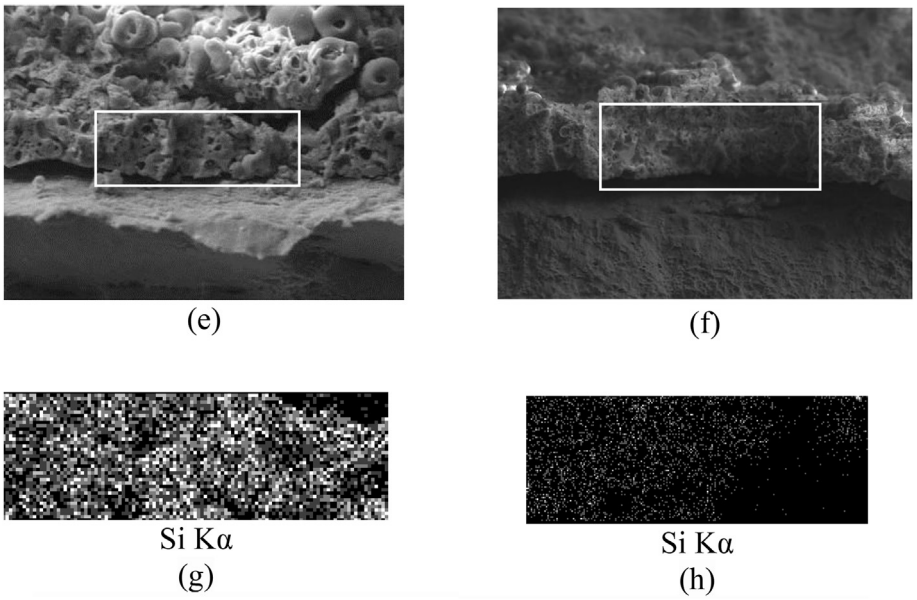

Fig. 6. SEM micrographs (e, f) and grey-level maps of Si distribution (g, h) in the W–CaP coating on Ti (e, g) and Zr–1Nb f, h) produced under 200 V.

(Fig. 8 c).

TEM study revealed the amorphous structure of the W-CaP coatings on Ti. Fig. 9 shows the bright–field (BF) and dark–field (DF) TEM images with selected–area diffraction (SAD) patterns of W–CaP coating particle removed from Ti substrate. Crystallites are not observed in the TEM images. In this case, two diffuse halo are observed in SAD pattern (Fig. 9c).

Fig. 10 shows IR–spectra of W–CaP coatings on Ti and Zr–1Nb. The strong bands at 1130–1030 cm^{-1} and 960–930 cm^{-1} belong to asymmetrical and symmetrical fluctuations of P–O phosphate

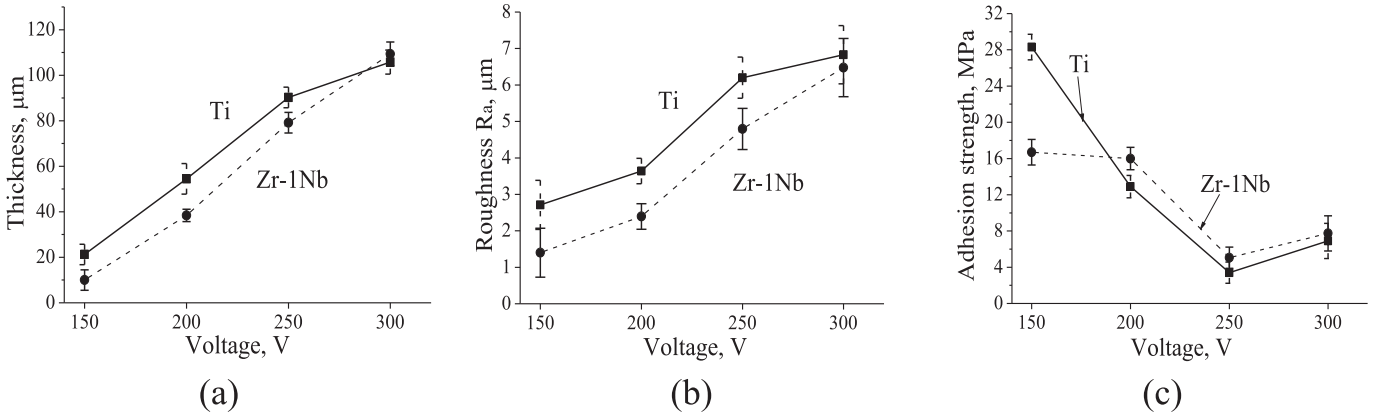

Fig. 7. Graphs of the thickness (a), surface roughness R_a (b) and adhesion strength (c) against the MAO voltage for the W–CaP coatings deposited on the Ti and Zr–1Nb.

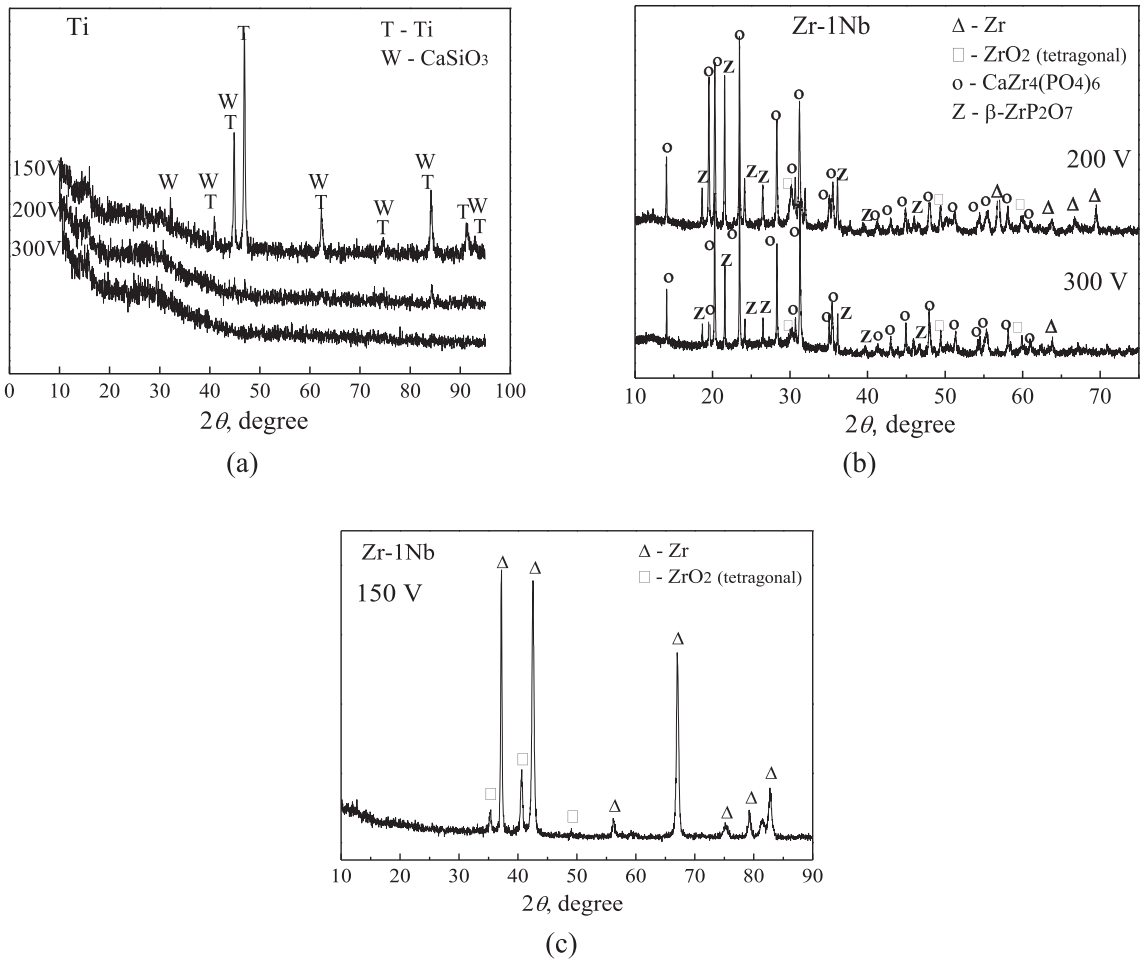

Fig. 8. XRD patterns of W–CaP coatings deposited on Ti (a) and Zr–1Nb (b, c) under different MAO voltages.

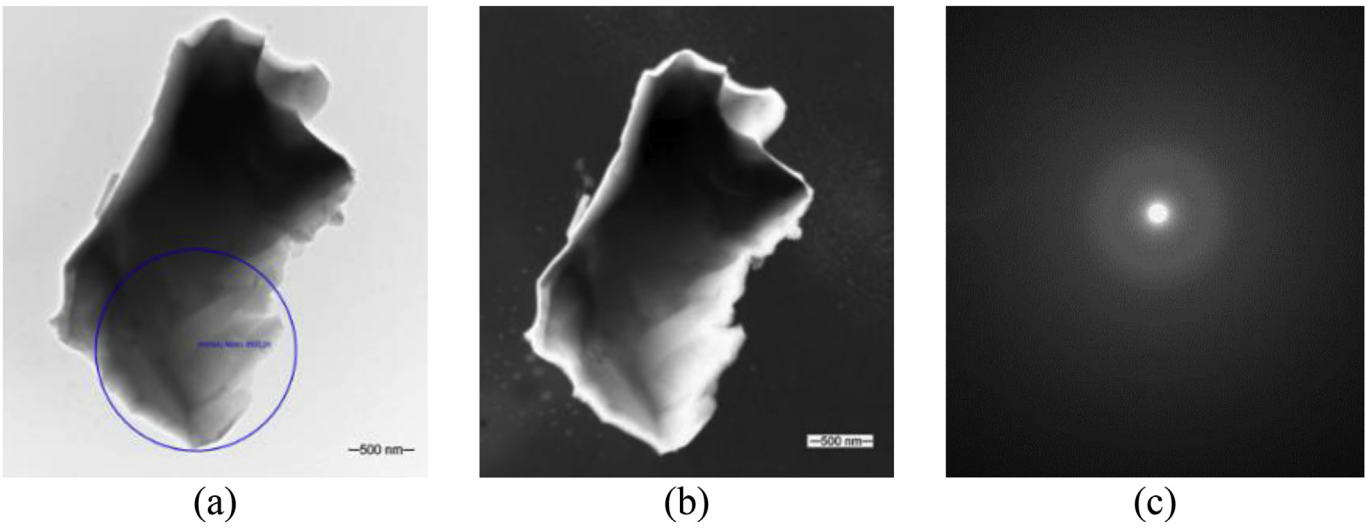

Fig. 9. BF–TEM (a) and DF–TEM (b) images with SAD pattern (c) for particle of W–CaP coating deposited on Ti under 300 V.

bonds, respectively. In addition the bands at 600–520 cm^{-1}, corresponding to triple–degenerated deformation oscillations of O–P–O bonds in the phosphate group are observed in these spectra [5]. The shoulder in the area of 800–730 cm^{-1} also indicates the presence of P–O–P bridge bonds. The bands in the area of 1420–1460 cm^{-1} correspond to the valence vibrations along the C–O bonds. It is due to the presence of carbonate impurities in wollastonite [21]. IR–spectra of W–CaP coating deposited on Ti

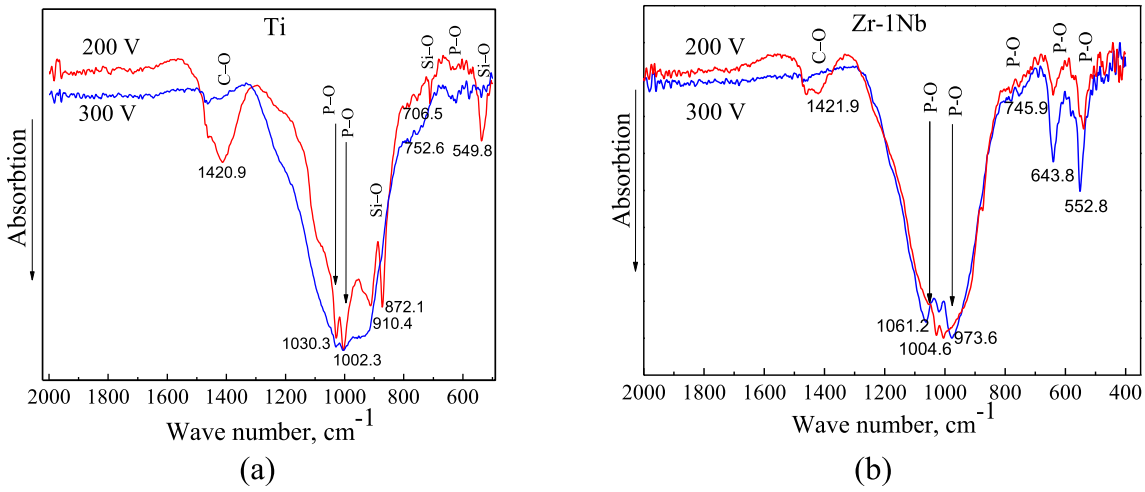

Fig. 10. IR–spectra of the W–CaP coatings deposited on Ti (a) and Zr–1Nb (b) under different process voltages.

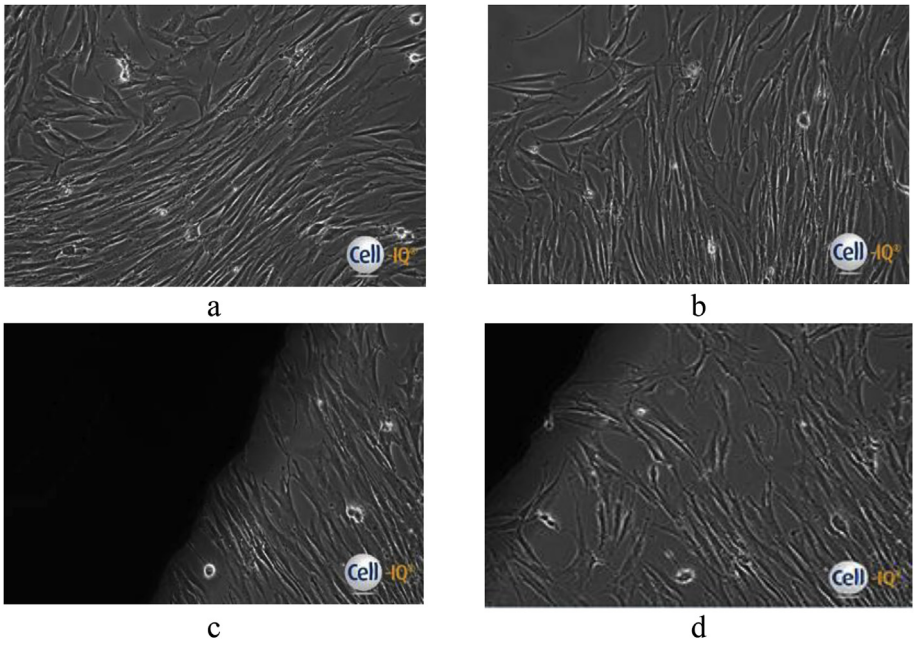

Fig. 11. Phase–contrast microscopy images of AMMSCs adhered to plastic wells (control group) (a, b), in the interfaces between the cells and W-CaP coating on Ti (c) and Zr–1Nb (d) after 7 day's culture; the dark field is a specimens with coatings.

Table 1
Viability of adipose–derived MMSCs in 7–day culturing either without (control) or with different substrates deposed by *W-CaP* coating, Me (Q1–Q3), n = 3.

The number of viable cells,%	
Ti substrate	Zr–1Nb substrate
87 (84–91) (control)	
91 (91–94)	93 (88–95)

under 200 V (Fig. 10a) shows the presence of the bands at 990–900 cm^{-1} and 750–550 cm^{-1} that belong to symmetrical fluctuations of the Si–O–Si bonds (inside the silica oxygen groups) and O–Si–O bonds (between the silicon–oxygen groups), respectively [21]. These bands disappear with increasing oxidation voltage from 200 to 300 V (Fig. 10a). Absorption bands for the coating deposited on Ti under 300 V are diffuse. The broad band of phosphate vibrations (1250–800 cm^{-1}) is observed. Thus, it was found by the XRD, SEM and TEM data and IR–spectra that the increase of the process voltage up to 300 V leads to the dissociation of the wollastonite. Fragments of the silicate structure were remained in the X-ray amorphous coating deposited on Ti under the 200 V. The structure of coatings on Zr–1Nb was presented by crystalline phases of phosphates and oxides.

In biological tests we observed the cell culture morphology using phase-contrast microscopy to investigate the biological activity of the coatings on Ti and Zr–1Nb. Some scientists consider a biocompatibility and functional activity of implants for osteosynthesis depend significantly on the processes taking place at the bone/implant interface [22]. Results of phase–contrast Cell–IQ microscopy *in situ* showed an absence of significant differences between morphological behavior of human AMMSCs in control

group (cell medium without specimens) as compared with W-CaP coated Ti and Zr-1Nb specimens (Fig. 11). The fibroblast–like cells adhered, increased cell mass and migrated actively to the monolayer formation. It indicates the high life activity and a motility of AMMSCs in the interface of "W-CaP coating/cells". Moreover, the developed W-CaP coatings on both substrates have no toxic effect (Table 1) on a viability of 7-day AMMSCs culture *in vitro*.

4. Conclusions

The investigations of structure, morphology, thickness, roughness and adhesion strength of the W–CaP coatings deposited by the MAO method under 130–300 V on the Ti and Zr–1Nb alloy were performed. The coatings were formed on the Ti with higher initial amplitude current than on Zr–1Nb. It can be explained by the differences between physical properties of TiO_2 and ZrO_2 oxides. The comparative investigations of W–CaP coatings showed the processes of the coatings formation on the Ti and Zr–1Nb alloy are similar in many respects. The identical dependencies of changes of the coating thickness, surface roughness and adhesion strength on the process voltage were revealed for the both substrates. Thin W–CaP coatings with the thickness of 10–15 μm were formed on Ti and Zr–1Nb under the low process voltage of 130–150 V. Elongated wollastonite particles with the size in the range of 40–100 μm were observed in such coatings. Thick porous coatings (40–110 μm) were formed on Ti and Zr–1Nb under the process voltages of up to the 300 V. In this case, spheres with pores were formed on the coating surface.

The structure of the coatings on Ti was presented by the X–ray amorphous and crystalline phases. The X–ray reflexes relating to Ti and wollastonite were observed only in XRD patterns of the thin coatings deposited under 130–200 V. The coatings formed on Zr–1Nb had the crystalline structure. The crystalline phases of $CaZr_4(PO_4)_6$, β–ZrP_2O_7, ZrO_2–tetragonal and Zr were detected. FT–IRS, XRD, SEM, and TEM data for W–CaP coatings confirmed that the increase of the oxidation voltage up to 300 V leads to the dissociation of the wollastonite. This could be due to the temperature increase in the micro–discharge areas during the MAO process. The developed W-CaP coatings on both substrates have no toxic effect on a viability, morphology and motility of AMMSCs culture *in vitro*.

Acknowledgements

The work was conducted as part of the program of fundamental researches of the state academies of sciences (PFR SAS) for 2015–2017 No.23.2.5, as well as RFBR grant № 15–03–07659 and project No. 16-15-10031 of Russian Science Foundation (in part of biological studies *in vitro*). The authors are grateful to A.I. Tolmachev, P.V. Uvarkin, T.V. Tolkacheva, K. A. Prosolov, I.A. Glukhov from the Institute of Strength Physics and Materials Science of SB RAS (Tomsk, Russia) for their assistance in carrying out of the research.

References

[1] M. Niinomi, M. Nakai, J. Hieda, Development of new metallic alloys for biomedical application, Acta Biomater. 8 (2012) 3888–3903, http://dx.doi.org/10.1016/j.jmbbm.2012.11.014.
[2] M.A.H. Gepreel, M. Niinomi, Biocompatibility of Ti–alloys for long–term implantation, J. Mech. Behav. Biomed. Mater. 20 (2013) 407–415, http://dx.doi.org/10.1016/j.jmbbm.2012.11.014.
[3] R. Kondo, N. Nomura, Suyalatu, Y. Tsutsumi, H. Doi, T. Hanawa, Microstructure and mechanical properties of as-cast Zr–Nb alloys, Acta Biomater. 7 (2011) 4278–4284, http://dx.doi.org/10.1016/j.actbio.2011.07.020.
[4] S. Liu, B. Li, C. Liang, H. Wang, Z. Qiao, Formation mechanism and adhesive strength of a hydroxyapatite/TiO_2 composite coating on a titanium surface prepared by micro-arc oxidation, Appl. Surf. Sci. 362 (2016) 109–114, http://dx.doi.org/10.1016/j.apsusc.2015.11.086.
[5] E.V. Legostaeva, Yu. P. Sharkeev, M. Epple, O. Prymak, Structure and properties of microarc calcium phosphate coatings on the surface of titanium and zirconium alloys, Russ. Phys. J. 56 (2014) 1130–1136, http://dx.doi.org/10.1007/s11182-014-0152-7.
[6] J.Y. Ha, Y. Tsutsumi, H. Doi, N. Nomura, K.H. Kim, T. Hanawa, Enhancement of calcium phosphate formation on zirconium by micro-arc oxidation and chemical treatments, Surf. Coat. Technol. 205 (2011) 4948–4955, http://dx.doi.org/10.1016/j.surfcoat.2011.04.079.
[7] S. Yu, Z. Yu, G. Wang, J. Han, X. Ma, M.S. Dargusch, Preparation and osteoinduction of active micro-arc oxidation films on Ti-3Zr-2Sn-3Mo-25Nb alloy, Trans. Nonferrous Metals Soc. China 21 (2011) 573–580, http://dx.doi.org/10.1016/S1003-6326(11)60753-X.
[8] M. Vert, Polymeric biomaterials: strategies of the past vs. strategies of the future, Prog. Polym. Sci. 32 (2007) 755–761, http://dx.doi.org/10.1016/j.progpolymsci.2007.05.006.
[9] A.L. Yerokhin, A. Shatrov, V. Samsonov, P. Shashkov, A. Leyland, A. Matthews, Fatigue properties of Keronite coatings on a magnesium alloy, Surf. Coat. Technol. 182 (2004) 78–84, http://dx.doi.org/10.1016/S0257-8972(03)00877-6.
[10] W. Simka, M. Sowa, R.P. Socha, A. Maciej, J. Michalska, Anodic oxidation of zirconium in silicate solutions, Electrochim. Acta 104 (2013) 518–525, http://dx.doi.org/10.1016/j.electacta.2012.10.130.
[11] M. Sowa, D. Łastówka, A.I. Kukharenko, D.M. Korotin, E.Z. Kurmaev, S.O. Cholakh, W. Simka, Characterisation of anodic oxide films on zirconium formed in sulphuric acid: XPS and corrosion resistance investigations, J. Solid State Electrochem. (2016) 1–8, http://dx.doi.org/10.1007/s10008-016-3369-2.
[12] Y. Yan, Y. Han, D. Li, J. Huang, Q. Lian, Effect of $NaAlO_2$ concentrations on microstructure and corrosion resistance of Al_2O_3/ZrO_2 coatings formed on zirconium by micro-arc oxidation, Appl. Surf. Sci. 256 (2010) 6359–6366, http://dx.doi.org/10.1016/j.apsusc.2010.04.017.
[13] A. Kazek-Kęsik, M. Krok-Borkowicz, E. Pamuła, W. Simka, Electrochemical and biological characterization of coatings formed on Ti–15Mo alloy by plasma electrolytic oxidation, Mater. Sci. Eng. C 43 (2014) 172–181, http://dx.doi.org/10.1016/j.msec.2014.07.021.
[14] A. Kazek-Kęsik, G. Dercz, K. Suchanek, I. Kalemba-Rec, J. Piotrowski, W. Simka, Biofunctionalization of Ti–13Nb–13Zr alloy surface by plasma electrolytic oxidation. Part I, Surf. Coat. Technol. 276 (2015) 59–69, http://dx.doi.org/10.1016/j.surfcoat.2015.06.034.
[15] A. Kazek-Kęsik, M. Krok-Borkowicz, A. Jakóbik-Kolon, E. Pamuła, W. Simka, Biofunctionalization of Ti–13Nb–13Zr alloy surface by plasma electrolytic oxidation. Part II, Surf. Coat. Technol. 276 (2015) 23–30, http://dx.doi.org/10.1016/j.surfcoat.2015.06.035.
[16] M.B. Sedelnikova, Yu.P. Sharkeev, E.G. Komarova, I.A. Khlusov, V.V. Chebodaeva, Structure and properties of the wollastonite–calcium phosphate coatings deposited on titanium and titanium–niobium alloy by the micro-arc oxidation method, Surf. Coat. Technol. 307 (2016) 1274–1283, http://dx.doi.org/10.1016/j.surfcoat.2016.08.062.
[17] M.B. Sedelnikova, E.G. Komarova, Yu.P. Sharkeev, T.V. Tolkacheva, Formation and properties of biocoatings based on wollastonite and calcium phosphates, AIP Conf. Proc. 1683 020202 (2015), http://dx.doi.org/10.1063/1.4932892.
[18] E.V. Legostaeva, K.S. Kulyashova, E.G. Komarova, M. Epple, Yu.P. Sharkeev, I.A. Khlusov, Physical, chemical and biological properties of micro-arc deposited calcium phosphate coatings on titanium and zirconium-niobium alloy, Mater. Werkst. 44 (2013) 188–197, http://dx.doi.org/10.1002/mawe.201300107.
[19] L.I. Tushinskiy, A.V. Plokhov, A.O. Tokarev, V.I. Sindeev, Methods for Investigations of Materials, Mir, Moscow, 2004.
[20] P.A. Zuk, M. Zhu, H. Mizuno, J. Huang, J.W. Futrell, A.J. Katz, P. Benhaim, H.P. Lorenz, M.H. Hedrick, Multilineage cells from human adipose tissue: implications for cell–based therapies, Tissue Eng. 7 (2001) 211–228, http://dx.doi.org/10.1089/107632701300062859.
[21] S. Rutstein, W.B. White, Vibrational spectra of high-calcium piroxenes and piroxenoids, Am. Mineralogist 56 (1971) 877–887.
[22] J.V. Nepola, C.A.J. Rockwood, D.P. Green, et al., External fixation, in: Rockwood and Green's Fractures in Adults V.1, fourth ed., Lippincott–Raven Publ., New York, 1996, pp. 229–304.